International Scientific Organization
http://iscientific.org/
Chemistry International
www.bosaljournals.com/chemint/

$Pb((SeP^iPr_2)_2N(S_2CNEt_2)$ complex to lead chalcogenide nanoparticles: A pyrolysis approach

Nathaniel Owusu Boadi[1*], Selina Ama Saah[2], Michael Baah Mensah[1], Johannes A. M. Awudza[1]

[1]Department of Chemistry, Kwame Nkrumah University of Science and Technology, Kumasi, Ghana
[2]Department of Chemical Sciences, University of Energy and Natural Resources, Sunyani, Ghana
*Corresponding author's E. mail: noboadi@gmail.com

ARTICLE INFO

Article type:
Research article
Article history:
Received January 2024
Accepted March 2024
July 2024 Issue
Keywords:
Pyrolysis
Lead chalcogenide nanoparticles
Single-source precursor
metal-organic complexes
Binary nanoparticles

ABSTRACT

This study investigated the use of a mixed ligand complex $[Pb((SeP^iPr_2)_2N(S_2CNEt_2)]$ as a single-source precursor for synthesizing lead chalcogenide nanoparticles through pyrolysis. The complex was decomposed under nitrogen gas at 600 °C for 30 minutes, and the residue was dispersed in toluene. Surprisingly, the resulting nanoparticles exhibited a cubic PbSe crystal structure based on their P-XRD pattern rather than the expected ternary alloy of PbS_xSe_{1-x}. SEM analysis showed that the nanoparticles grew in clusters of cubes with an average size of 119 nm. EDX also confirmed the formation of binary PbSe nanoparticles rather than a ternary PbS_xSe_{1-x} alloy. The pyrolysis route found to be highly promising for the synthesis of pure lead chalcogenide nanoparticles.

Capsule Summary: A mixed-ligand complex as a precursor for lead chalcogenide nanoparticle synthesis through pyrolysis was investigated. The complex was decomposed at 600 °C under nitrogen, yielding cubic PbSe nanoparticles instead of the expected ternary alloy.

Cite This Article As: N. O. Boadi, S. A. Saah, M. B. Mensah, J. A. M. Awudza. $Pb((SeP^iPr_2)_2N(S_2CNEt_2)$ complex to lead chalcogenide nanoparticles: A pyrolysis approach. Chemistry International 10(3) (2024) 75-80.
https://doi.org/10.5281/zenodo.11003972

INTRODUCTION

Metal-organic complexes have been used as single-source precursors for synthesizing semiconducting nanomaterials such as metal sulfides, selenides, and oxides. This is due to their numerous advantages over dual and multi-source synthetic precursors (Batool et al., 2022; Boadi et al., 2012, 2016, 2019; Boadi, Saah, Mensah, et al., 2020; Kotei et al., 2022; Kshirsagar and Khanna, 2022; Saah, Boadi, Awudza, et al., 2022; Saah, Boadi and Awudza, 2022; Saah, Boadi and Wilkins, 2019; Saah, Boadi, Adu-Poku, et al., 2019). These advantages include the following: (i) the single-source precursor produces the target compound with perfect stoichiometry; (ii) the reaction process involving these single-source precursors is cleaner, less toxic, and easily handled; (iii) they produce pure crystalline materials, and their decomposition pathways occur at low temperatures (100-300 °C) (Batool et al., 2022; Malik et al., 2010; Saah, Boadi and Wilkins, 2019).

Unlike CdS and ZnS, which have wide bandgaps of 2.4 and 3.6 eV, respectively (Thomas et al., 2015), lead chalcogenides are narrow bandgap semiconducting materials (PbSe = 0.27 eV and PbS = 0.41 eV) (Saah et al., 2018). They are crystalline with cubic geometry and can form p-type or n-type semiconductors (Afzaal and O'Brien, 2006; Rathore et

al., 2022; Yu et al., 2022). They absorb the electromagnetic spectrum's infrared region in their bulk state, making them useful in photoconductive infrared detectors (Saah et al., 2019, Miao et al., 2022). PbS and PbSe nanocrystals with similar bandgaps generate large short-circuit current and open-circuit voltage (Saha et al., 2015, Ahmad et al., 2019). However, forming a ternary alloy of PbS_xSe_{1-x} could lead to engineered nanoparticles that optimize both voltage and carrier transport (Cai et al., 2022; Nam et al., 2012; Saah et al., 2017). This study adds to the limited research using single-source precursors for synthesizing ternary PbS_xSe_{1-x} nanomaterials (Saah et al., 2017). This research aims to synthesize and characterize lead chalcogenide nanoparticles from $[Pb((SeP^iPr_2)_2N(S_2CNEt_2)]$ complex using the pyrolysis method. Contrary to the expectation of forming a ternary alloy, PbSe nanoparticles were produced and characterized by various techniques.

MATERIAL AND METHODS

Chemicals and reagents

Chlorodiisopropyl phosphine, lead acetate, selenium powder and sodium diethyldithiocarbamate were procured for Sigma-Aldrich, UK and used as received to synthesize the precursors. The dry toluene was obtained from the solvent purification system at the School of Chemistry, University of Manchester, UK. Standard reported procedures were followed to synthesize $[Pb((SeP^iPr_2)_2N)_2]$ and $[Pb(S_2CNEt_2)_2]$ (Cupertino et al., 1999). The synthesis of the $[Pb((SeP^iPr_2)_2N(S_2CNEt_2)]$ complex is described in our earlier study and the same was adopted in the present investigation (Saah and Awudza, 2020).

Instrumentation

The P-XRD analysis was conducted using a Bruker AXS D8 diffractometer equipped with a Cu-Kα radiation source (λ =1.5418 Å at 40 kV and 40mA at room temperature). The nanoparticles were scanned from 20 to 80° 2-theta with a step size of 0.02° and a dwell time of 3 seconds. The morphology of the nanoparticles and their elemental composition were determined using a Philips (FEG) XL 30 scanning electron microscope (SEM) equipped with a DX4 energy-dispersive X-ray (EDX) detector. Before the SEM and EDX analyses, the samples were carbon-coated using an Edwards coating system E306A.

Pyrolysis of $[Pb((SeP^iPr_2)_2N(S_2CNEt_2)]$

A mass of 6.4 mg (0.084 mmol) of the $[Pb((SeP^iPr_2)_2N(S_2CNEt_2)_2)]$ complex was weighed into a stainless-steel crucible and pyrolyzed in a carbolite furnace at 600 °C for 1 hour under nitrogen gas. The black powdery residue of 2.36 mg was dispersed in toluene and sonicated for 1 hour in an ultrasonic bath.

RESULTS AND DISCUSSION

The decomposition behavior of $[Pb((SeP^iPr_2)_2N(S_2CNEt_2))]$ was investigated using thermogravimetric analysis under a nitrogen atmosphere with a heating rate of 10 °C/min. The analysis revealed a two-step weight loss between 273.14 and 376 °C. The estimated residual weight loss for bulk PbSxSe1−x was 34.5%. However, based on the residual material (33.2%) obtained from the TGA experiments, the final product was within 4% of the expected residual weight loss (Boadi, Saah, and Awudza, 2020). The complex exhibited a distorted octahedral geometry with a monoclinic crystal system and a P2 (1)/n space group (Boadi, Saah, and Awudza, 2020).

Powder XRD of pyrolysed $[Pb((SeP^iPr_2)_2N(S_2CNEt_2))]$ complex

Based on the powder XRD analysis (Figure 1), the pyrolyzed sample formed a cubic PbSe phase instead of the expected PbS_xSe_{1-x}. The d-spacing values obtained for PbSe nanoparticles match the standard ICDD 04-004-4328, and the intense (200) peak suggests a (200) oriented growth with a crystallite size of 11.41 nm. Additionally, the sharpening of the peaks confirms the high crystallinity of the PbSe nanoparticles. The DFT calculations suggest that the formation of PbSe might involve more than one mechanism. However, the steps leading to the formation of PbSe are more favorable on thermodynamic grounds than those leading to PbS formation (Akhtar et al., 2011). These findings are consistent with previous studies on decomposing mixed ligand single-source lead complexes (Boadi et al., 2019; Boadi, Saah and Awudza, 2020; Boadi, Saah, Mensah, et al., 2020). The calculated lattice constant 'a' for the PbSe phase was 6.1324 Å.

SEM analysis of pyrolyzed $[Pb((SeP^iPr_2)_2N)(S_2CNEt_2))]$

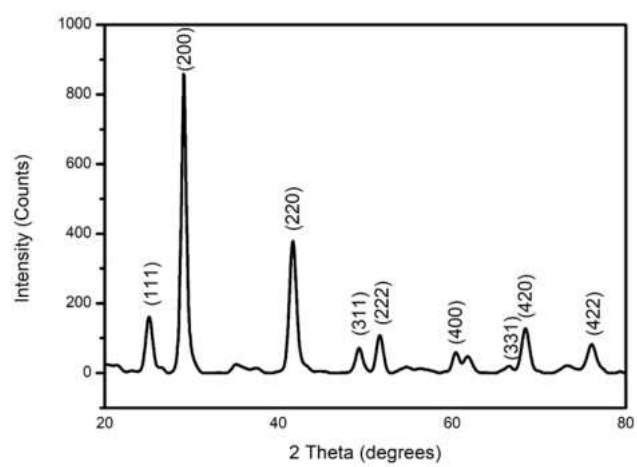

Fig. 1: P-XRD of PbSe nanoparticles from $[Pb((SeP^iPr_2)_2N)(S_2CNEt_2))]$ complex

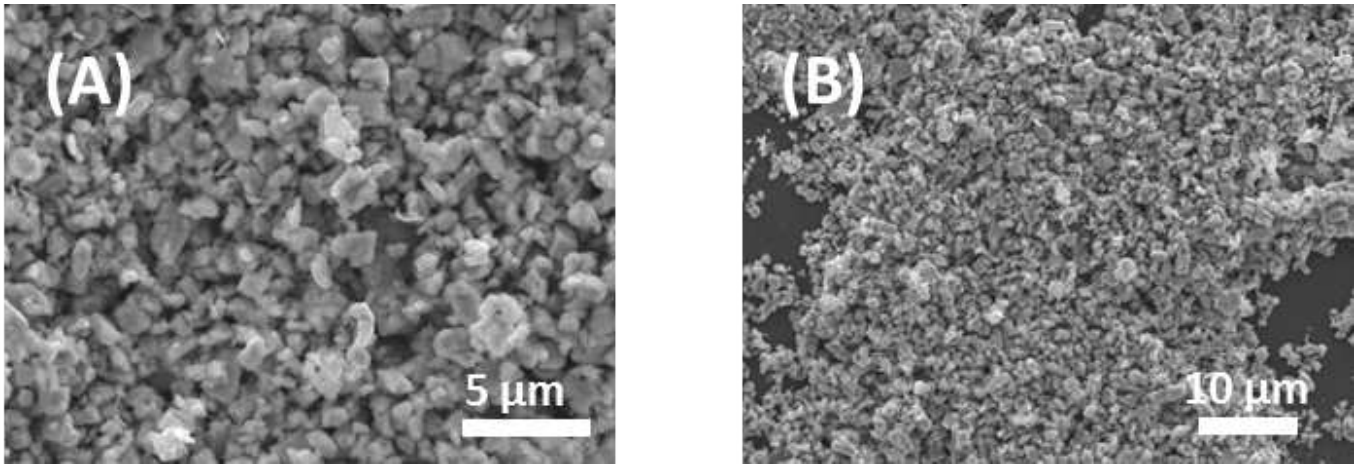

Fig. 2: SEM images of PbSe nanoparticles from $[Pb((SeP^iPr_2)_2N(S_2CNEt_2))]$ complex at (A) 5000x and (B) 2000x magnification

The obtained SEM images (Figure 2) provided a comprehensive visual representation, revealing intriguing insights into the structural characteristics of the nanoparticles under investigation. The analysis of these images unveiled clusters of cubic PbSe crystals, which exhibited a notable absence of any discernible regular arrangement or specific order. This observation suggests that the nanoparticles possess a highly disordered internal structure, indicating the absence of a well-defined crystal lattice arrangement (Song and Cölfen, 2010).

As revealed by the SEM analysis, the particle size distribution exhibited a considerable range, spanning from 38.8 to 727.4 nm with an average particle size of 119.7 nm. These results highlight the significant heterogeneity within the sample, indicating the presence of particles of varying sizes (Rabanel et al., 2019).

The structural characteristics and particle size distribution of the PbSe nanoparticles obtained from this study are consistent with prior research conducted in this field (Begum et al., 2012; Cui et al., 2005; Malik et al., 2014). These studies have consistently demonstrated that PbSe nanoparticles tend to undergo rapid agglomeration, leading to polycrystalline materials characterized by larger particle sizes. The wide particle size distribution observed in this study further underscores the complex nature of the agglomeration process and highlights the need for careful control and characterization of nanoparticle systems in future applications (Bavykina et al., 2020).

The energy-dispersive X-ray spectroscopy (EDX) analysis of the thin film in Figure 3 revealed the absence of sulfur, which cannot be detected in PbSxSe1−x due to the overlapping of the selenium K line and the lead M5 absorption edge (Akhtar et al., 2011). The composition of the film was 72.03% Pb and 27.82% Se, with a slight trace of phosphorus (0.15%). The high lead content (>50%) contributes to the high crystallinity of the PbSe nanoparticles (Thanikaikarasan et al., 2012).

The detection of phosphorus is not surprising, as its contamination during the decomposition of phosphorus-containing complexes is expected at higher temperatures (6-9%) and lower temperatures (1-2%) (Akhtar *et al.*, 2011). The higher thermodynamic stability of selenium over sulfur could be a reason why PbSe formed instead of PbSxSe1-x, as the high pyrolysis temperature of 600 °C provides enough energy for selenium to form a stable compound with lead (Akhtar et al., 2011; Saah et al., 2017).

A novel precursor, $Pb((SeP^iPr_2)_2N(S_2CNEt_2)$ was introduced for synthesizing lead chalcogenide nanoparticles. This expands the range of available precursors for nanoparticle synthesis, potentially offering advantages such as improved control over nanoparticle properties or simplification of the synthesis process.

The utilization of the $Pb((SeP^iPr_2)_2N(S_2CNEt_2)$ complex as a precursor for synthesizing lead chalcogenide nanoparticles via pyrolysis. The resulting nanoparticles exhibit a cubic PbSe crystal structure instead of the expected ternary alloy of PbS_xSe_{1-x}. SEM analysis reveals clustered cubic nanoparticles with an average size of 119 nm. EDX confirms the formation of binary PbSe nanoparticles instead of a ternary PbS_xSe_{1-x} alloy. Lead chalcogenide nanoparticles have various applications in fields such as optoelectronics, photovoltaics, and thermoelectric due to their unique electronic and optical properties (Ashraf et al., 2016; Esakkiraj et al., 2015; Priyadharsini et al., 2016). Understanding alternative synthesis routes and the resulting nanoparticle properties could lead to the development of new or improved devices. Hence, this study contributes to the advancement of nanoparticle synthesis methodologies, provides insights into crystal structure formation, and holds potential implications for various technological applications.

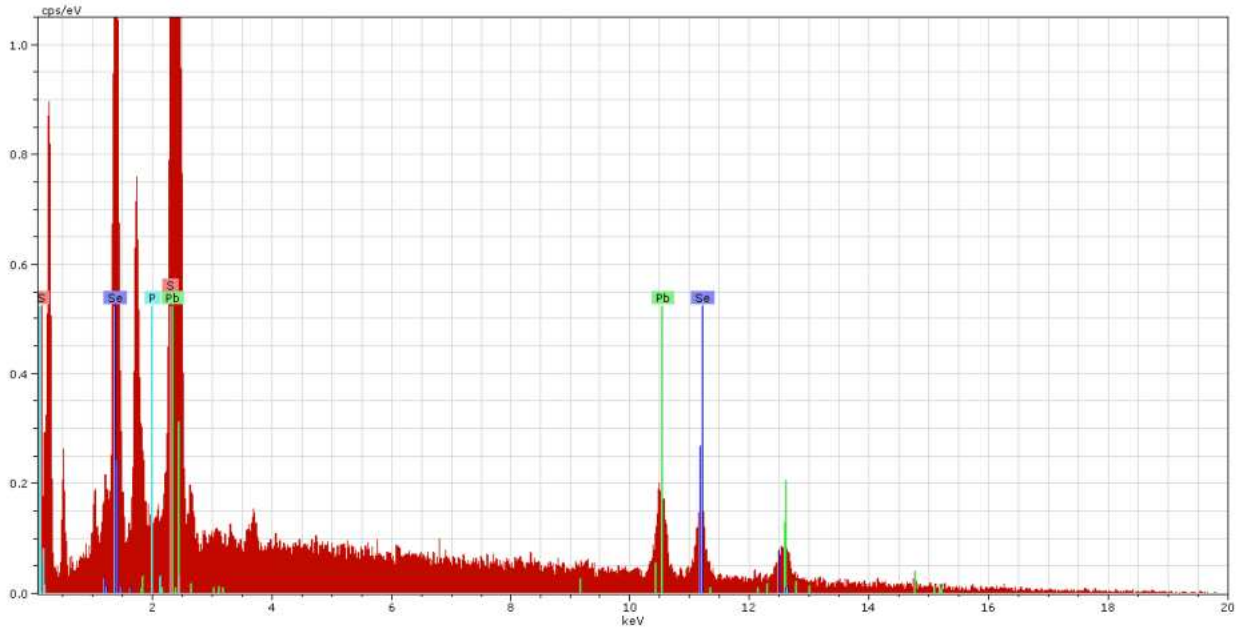

Fig. 3: EDX spectrum of PbSe nanoparticles from $[Pb((SeP^iPr_2)_2N(S_2CNEt_2)_2)]$ complex

CONCLUSIONS

In this study, lead chalcogenide nanoparticles were synthesized using a pyrolysis method employing the precursor $[Pb((SeP^iPr_2)_2N(S_2CNEt_2)]$. The synthesized nanoparticles were subjected to characterization through various techniques, namely powder X-ray diffraction (P-XRD), scanning electron microscopy (SEM), and energy-dispersive X-ray spectroscopy (EDX). The P-XRD analysis provided valuable insights into the crystal structure of the synthesized nanoparticles. The results revealed the formation of cubic PbSe nanoparticles, as evidenced by characteristic diffraction peaks corresponding to the ICDD No. 04-004-4328 pattern. To further investigate the elemental composition of the synthesized nanoparticles, EDX analysis was performed. The EDX analysis demonstrated the absence of sulfur within the nanoparticles, confirming the pure formation of PbSe. However, during the EDX analysis, a small amount of phosphorus was detected. This phosphorus signal likely originated from the decomposition of the precursor complex $[Pb((SeP^iPr_2)_2N(S_2CNEt_2)]$.

DECLARATION OF COMPETING INTEREST

The authors declare no competing financial interest.

ACKNOWLEDGEMENTs

The writers gratefully acknowledge the Royal Society Leverhulme Africa Award Program (London). Prof. Paul O'Brien, FRS, CBE, of blessed memory, is deeply appreciated by the writers for his tremendous assistance and direction in this study.

REFERENCES

Afzaal, M., O'Brien, P., 2006. Recent developments in II–VI and III–VI semiconductors and their applications in solar cells. Journal of Materials Chemistry 16, 1597-1602.

Ahmad, W., He, J., Liu, Z., Xu, K., Chen, Z., Yang, X., Li, D., Xia, Y., Zhang, J., Chen, C., 2019. Lead Selenide (PbSe) Colloidal Quantum Dot Solar Cells with >10% Efficiency. Advanced Materials 31, 1–24.

Akhtar, J., Afzaal, M., Vincent, M.A., Burton, N.A., Raftery, J., Hillier, I.H., O'Brien, P., 2011. Understanding the Decomposition Pathways of Mixed Sulfur/Selenium Lead Phosphinato Complexes Explaining the Formation of Lead Selenide. The Journal of Physical Chemistry C 115, 16904–16909.

Ashraf, M.T., Salah, N.A., Rafat, M., Zulfequar, M., Khan, Z.H., 2016. Optical studies on Zn-doped lead chalcogenide (PbSe)100−xZnx thin films composed of nanoparticles. Thin Solid Films 612, 109-115.

Batool, M., Gill, R., Munawar, K., McKee, V., Mazhar, M., 2022. Single source precursor derived ZnO–PbO composite thin films for enhanced photocatalytic activity. Journal of Solid State Chemistry 305, 122642–122651.

Bavykina, A., Kolobov, N., Khan, I.S., Bau, J.A., Ramirez, A., Gascon, J., 2020. Metal-Organic Frameworks in Heterogeneous Catalysis: Recent Progress, New Trends, and Future Perspectives. Chemical Reviews 120, 8468–8535.

Begum, A., Hussain, A., Rahman, A., 2012. Effect of deposition temperature on the structural and optical properties of chemically prepared nanocrystalline lead selenide thin films. Beilstein Journal of Nanotechnology 3, 438–443.

Boadi, N.O., Malik, M.A., O'Brien, P., Awudza, J.A.M., 2012. Single source molecular precursor routes to lead chalcogenides. Dalton transactions 41, 10497–10506.

Boadi, N.O., McNaughter, P.D., Helliwell, M., Malik, M.A., Awudza, J.A.M., O'Brien, P., 2016. The Deposition of PbS and PbSe Thin Films from Lead Dichalcogenoimidophosphinates by AACVD. Inorganica Chimica Acta 453, 439–442.Boadi, N.O., Saah, S.A., Awudza, J.A.M., 2020a. Synthesis of a novel single-source precursor for the production of lead chalcogenide thin films. Journal of Chemistry 2020, 1–7.

Boadi, N.O., Saah, S.A., Helliwell, M., Awudza, J.A.M., 2019. Hot-Injection Synthesis of PbE (E= S, Se) Nanoparticles from Dichalcogenoimidophosphinato Lead (II) Complexes. ChemistrySelect 4, 13908–13911.

Boadi, N.O., Saah, S.A., Mensah, M.B., Awudza, J.A.M., 2020b. Aerosol-Assisted Chemical Vapour Deposition of Lead Chalcogenide Thin Films from [Pb((SePiPr2)2N)(S2CNHexMe)]. Advances in Materials Science and Engineering 2020, 1–7.

Cai, B., Zhao, Y., Xu, D., Ouyang, G., 2022. Optimized photoelectric conversion properties of PbSxSe1- x-QD/MoS2-NT 0D-1D mixed-dimensional van der Waals heterostructures. New Journal of Physics 24, 1–11.

Cui, J., Guo, F., Liu, X., 2005. Morphology-controllable Solution Route to PbSe Micrometer-scaled Crystals. Chemistry Letters 34, 170–171.

Cupertino, D., Birdsall, D.J., Slawin, A.M.Z., Woollins, J.D., 1999. The preparation and coordination chemistry of Pr2P(E) NHP(E')iPr2(E, E'=Se; E=Se, E'=S; E=S, E'=O; E, E'=O. Inorganica Chimica Acta 290, 1–7.

Esakkiraj, E., Mohanraj, K., Sivakumar, G., Henry, J., 2015. On the optical properties of lead chalcogenide nanoparticles. Optik - International Journal for Light and Electron Optics 126, 2133-2137.

Kotei, P.A., Boadi, N.O., Saah, S.A., Mensah, M.B., 2022. Synthesis of Nickel Sulfide Thin Films and Nanocrystals from the Nickel Ethyl Xanthate Complex. Advances in Materials Science and Engineering 2022, 1–10.

Kshirsagar, A.S., Khanna, P.K., 2022. Ternary metal selenides by use of 4-nitroacetophenone selenosemicarbazone: Application of selenium Schiff base in nanotechnology. Inorganic Chemistry Communications 139, 109334–109346.

Malik, M.A., Afzaal, M., O'Brien, P., 2010. Precursor chemistry for main group elements in semiconducting materials. Chemical reviews 110, 4417–46.

Malik, S.N., Akhtar, M., Revaprasadu, N., Qadeer, A., Malik, M.A., 2014. Dialkyldiselenophosphinato-metal complexes – a new class of single source precursors for deposition of metal selenide thin films and nanoparticles. Materials Science and Engineering 64, 1–9.

Miao, M., Wang, Z., Guo, Z., Yan, G., Xing, J., 2023. Lattice-matched quantum-dots-perovskite solid-sol for the ultrafast, ultrasensitive and ultrastable uncooled photoconductive near-infrared sensor with simple structure. Ceramics International 49, 8148–8154.

Nam, M., Kim, S.S.-W.S.S., Kang, M., Kim, S.S.-W.S.S., Lee, K.-K., 2012. Efficiency enhancement in organic solar cells by configuring hybrid interfaces with narrow bandgap PbSSe nanocrystals. Organic Electronics 13, 1546–1552.

Priyadharsini, N., Vairam, S., Thamilselvan, M., 2016. Structural and optical properties of neodymium doped lead chalcogenide (PbSe) nanoparticles. Optik 127, 5046-5049

Rabanel, J.M., Adibnia, V., Tehrani, S.F., Sanche, S., Hildgen, P., Banquy, X., Ramassamy, C., 2019. Nanoparticle heterogeneity: An emerging structural parameter influencing particle fate in biological media? Nanoscale 11, 383–406.

Rathore, E., Juneja, R., Sarkar, D., Roychowdhury, S., Kofu, M., Nakajima, K., Singh, A.K., Biswas, K., 2022. Enhanced covalency and nanostructured-phonon scattering lead to high thermoelectric performance in n-type PbS. Materials Today Energy 24, 100953–100961.

Saah, S A, Boadi, N.O., Adu-Poku, D., Wilkins, C., 2019. Lead ethyl dithiocarbamates : efficient single-source precursors to PbS nanocubes. Royal Society Open Science 6, 1–8.

Saah, Selina A., Boadi, N.O., Awudza, J.A.M., 2022. Facile synthesis of PbS, Bi2S3 and Bi-doped PbS nanoparticles from metal piperidine dithiocarbamates complexes. Results in Chemistry 4, 100618.

Saah, Selina Ama, Boadi, N.O., Awudza, J.A.M., Revaprasadu, N., 2022. Structural influence of nitrogen adducts on the morphology of bismuth sulfide thin films. MRS Advances 7, 757–762.

Saah, Selina Ama, Boadi, N.O., Wilkins, C., 2019a. Deposition of PbS Thin Films from Lead Hexadecyl and Octadecyl Xanthate Complexes Using the Spin Coating Method. MRS Advances 4, 733–742.

Saah, Selina Ama, Khan, M.D., Awudza, J.A.M., Revaprasadu, N., O'Brien, P., 2019b. A Facile Green Synthesis of Ultranarrow PbS Nanorods. Journal of Inorganic and Organometallic Polymers and Materials 29, 2274–2281.

Saah, Selina A., McNaughter, P.D., Malik, M.A., Awudza, J.A.M., Revaprasadu, N., O'Brien, P., 2018. PbSxSe1−x thin films from the thermal decomposition of lead(II) dodecylxanthate and bis(N,N-diethyl-N′-naphthoylselenoureato)lead(II) precursors. Journal of Materials Science 53, 4283–4293.

Saha, S.K., Bera, A., Pal, A.J., 2015. Improvement in PbS-based hybrid bulk-heterojunction solar cells through band alignment via bismuth doping in the nanocrystals. ACS Applied Materials and Interfaces 7, 8886–8893.

Song, R.Q., Cölfen, H., 2010. Mesociystals - Ordered nanoparticle superstructures. Advanced Materials 22, 1301–1330.

Thanikaikarasan, S., Mahalingam, T., Dhanasekaran, V., Kathalingam, a., Rhee, J.-K., 2012. Growth and characterization of lead selenide thin films. Journal of Materials Science: Materials in Electronics 23, 1562–1568.

Thomas, P.J., Stansfield, G.L., Komba, N., Cant, D.J.H., Ramasamy, K., Albrasi, E., Al-Chaghouri, H., Syres, K.L., O'Brien, P., Flavell, W.R., Mubofu, E., Bondino, F., Magnano, E., 2015. Growth of nanocrystalline thin films of metal sulfides [CdS, ZnS, CuS and PbS] at the water–oil interface. RSC Advances 5, 62291–62299.

Yu, Z., Yao, Y., Yao, J., Zhang, L., Chen, Z., Gao, Y., & Luo, H., 2022. Raising the solubility of Gd yields superior thermoelectric performance in n-type PbSe. Journal of Materials Chemistry A 10, 20386–20395.